SCISPACE formerly Typeset

Open access • Journal Article • DOI:10.1116/1.1493785

Electronic states at the interface of Ti–Si oxide on Si(100) — Source link

C. C. Fulton, Gerald Lucovsky, Robert J. Nemanich

Institutions: North Carolina State University

Published on: 06 Aug 2002 - Journal of Vacuum Science & Technology B (American Vacuum Society)

Topics: Band gap, Semimetal, High-κ dielectric, Oxide and Photoemission spectroscopy

Related papers:

- High-κ gate dielectrics: Current status and materials properties considerations
- Band offsets of wide-band-gap oxides and implications for future electronic devices
- Process-dependent band structure changes of transition-metal (Ti,Zr,Hf) oxides on Si (100)
- Photoemission study of energy-band alignments and gap-state density distributions for high-k gate dielectrics
- MOSFET transistors fabricated with high permitivity TiO/sub 2/ dielectrics

Share this paper:

View more about this paper here: https://typeset.io/papers/electronic-states-at-the-interface-of-ti-si-oxide-on-si-100-57inrsy7v7

Electronic states at the interface of Ti–Si oxide on Si(100)

C. C. Fulton, G. Lucovsky, and R. J. Nemanich
Department of Physics, North Carolina State University, Raleigh, North Carolina 27695-8202

(Received 1 February 2002; accepted 18 May 2002)

The requirement for high K dielectrics for Si devices includes both a low interface state density and a band alignment that blocks both electrons and holes. Titanium dioxide materials are known to exhibit dielectric constants of 80 or higher depending on the crystal structure and, as such, are prime candidates for gate dielectrics. We employ an ultrathin layer of SiO_2 prior to the formation of a Ti oxide to limit the density of defect states. The electronic structure is observed during the stepwise growth of the oxide using x-ray and ultraviolet photoemission spectroscopy. Measurements indicate Ti oxide states at approximately 2 eV below the Si valence band maximum suggesting that the TiO_2 conduction band aligns with the Si conduction band. The results indicate nearly flat bands in the silicon consistent with a low interface state density. © *2002 American Vacuum Society.*
[DOI: 10.1116/1.1493785]

I. INTRODUCTION

With the ever shrinking dimensions of integrated devices and the desire for every possible reduction in switching time, the use of SiO_2 as a gate oxide is being pushed to its limits. To increase the sheet charge density in the channel, the capacitance must be increased. For a given material this is typically achieved by reducing the thickness of the gate dielectric. As the gate dielectric thickness is reduced below 2 nm, direct tunneling between the gate and channel becomes significant, leading to increased power consumption. One solution is to employ a high K material, allowing increased capacitance with thicker layers, thereby reducing the tunneling current characteristics.

The gate dielectric should have a low interface state density, a low number of trapped charges, and a band alignment that presents an effective barrier to both electrons and holes. For instance, with a band gap of ~ 8.9 eV, SiO_2 exhibits type I band alignment with Si, with a valence band offset of 4.5 eV and a conduction band offset of 3.3 eV.[1] Transition metal oxides are known to exhibit dielectric constants much higher than that of SiO_2, but the reactivity of the transition metals leads to an interface with a high density of interface states. One alternative is to employ an ultrathin layer of SiO_2 as a buffer between the transition metal oxide and the Si, as suggested by Campbell *et al.*[2] and Smith *et al.*[3]

Titanium dioxide has potentially useful characteristics as a gate dielectric. Rutile TiO_2 displays a dielectric constant of 80 and a band gap of 3.1 eV. For thin TiO_2 films, the dielectric constant has been measured to be between 8 and 70 (Ref. 4) with a band gap in the range of 3.0 to 4.9 eV, depending on phase and preparation technique.[4,5]

The electronic properties of TiO_2 films grown on Si were studied starting with a thin SiO_2 layer on Si(100), then depositing and oxidizing Ti metal films in a stepwise fashion. Electronic states are explored with x-ray and ultraviolet photoemission spectroscopy (XPS and UPS). From these measurements we construct schematic diagrams of the interface band structure evolution, tracing development from the oxidized Si through the formation of a mostly TiO_2 film.

II. EXPERIMENTAL PROCEDURES

The experiments presented here are accomplished in an integrated ultrahigh vacuum (UHV) system with interconnected but compartmentalized surface processing, film deposition, and surface characterization systems. The system involves a linear UHV transfer chamber that is ~ 13 m long and interconnects 13 different process and characterization systems. In this study, the following techniques are employed: remote plasma enhanced oxidation, electron beam evaporation for Ti metal, Auger electron spectroscopy (AES) for chemical analysis, x-ray photoelectron spectroscopy (XPS) for core levels, and ultraviolet photoelectron spectroscopy (UPS) for valence band spectra.

All of the studied structures are grown on 25 mm n-type silicon wafers oriented (100) and doped to 4×10^{16} donors per cm^2. Prior to loading into UHV, wafers are cleaned using a JT Baker 100 chemical dip for 15 min at room temperature, followed by 1 min of rinsing in deionized water. After transfer into UHV, the surfaces are characterized by AES then further cleaned by a 30 s exposure to remotely excited oxygen plasma. The remote plasma process effectively removes hydrocarbons and passivates the Si surface with a thin layer of SiO_2, as shown by Yasuda *et al.*[6]

The O_2 plasma clean and subsequent oxidations are carried out in a remote plasma enhanced chemical vapor deposition (RPECVD) chamber with base pressure of 3×10^{-9} Torr. Plasma exposures take place under the following conditions: 300 °C wafer surface temperature, 60 mTorr partial pressure of oxygen, gas flow 10 standard cubic centimeters per minute (sccm) O_2, and 50 sccm helium with 20 W rf power exciting the plasma. Plasma treatments differ only in exposure time, 30 s for cleaning and 30 s for each 0.2 nm of titanium that is to be oxidized. The cleaned wafer is studied again by AES, as well as by XPS and UPS. This gives a baseline for comparing the Ti and TiO_2 thin films.

X-ray characterization is performed at a pressure of 2×10^{-9} Torr using the 1253.6 eV Mg $K\alpha$ line from a Fisons XR3 dual anode source and a Fisons Clam II analyzer operated at 0.1 eV resolution. Observation "windows" are set

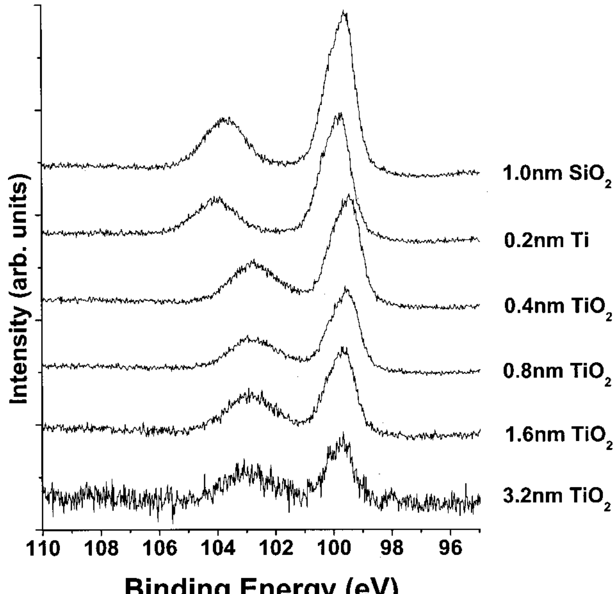

FIG. 1. Silicon $2p$ core levels for the prepared surface, initial metal film, and titanium oxides. The sequence runs top to bottom and the labels indicate the total film thickness deposited on SiO_2. The bulk Si (right) is shown to move away from flat band energy and slowly return as the total oxide thickness increases. Whereas bound Si (left) displays an overall chemical shift (3.2 nm TiO_2) as well as smaller shifts due to the intermediate Ti silicate in which the SiO_2 layer on the wafer is converted into a Ti silicate alloy.

around the Si $2p$, O $1s$, and Ti $2p$ binding energies to allow observation of the core level shifts. Ultraviolet photoemission spectra are obtained using the He I line at 21.2 eV in a chamber with base pressure 3×10^{-10} Torr. The VSW 50 mm mean radius hemispherical analyzer and VSW HAC300 give an electron energy resolution of 0.15 eV. A negative 4.00 V bias is applied to the substrate to overcome the analyzer work function.

Titanium metal is deposited by electron beam evaporation with a Sycon Instruments STM-100 crystal rate/thickness monitor providing thickness measurements. The deposition chamber is equipped with a shutter allowing a stable deposition rate to be established (by averaging total accumulated thickness over 1 min), then opening the shutter for the prescribed duration.

Metal films are deposited in steps of 0.2, 0.2, 0.4, and 0.8 nm (for a total deposition of 1.6 nm). Oxidation times are varied proportionally: 30, 30, 60, and 120 s for the respective metal film thickness.

III. RESULTS

The experimental process involves the formation of a thin oxide layer on Si(100), followed by the sequential deposition of Ti and low temperature plasma oxidation. The results of XPS and UPS spectra of the various steps are shown in Figs. 1–5.

The development of the Si $2p$ core level is displayed in Fig. 1. The scan of the oxidized surface shows peaks at 99.7 and 103.7 eV that are attributed to the bulk Si near the interface and the oxidized Si in the SiO_2, respectively. Shifts in the bulk Si feature are attributed to band bending in the Si substrate. An important point is the position of the final state of the bulk Si $2p$ core level; it is essentially unchanged from the original value. Small shifts are observed first to higher binding energy ($\sim$0.2 eV) after the deposition of the Ti layer, then to lower binding energies after oxidation.

The initial silicon dioxide thickness can be calculated by comparing the relative XPS intensities of the Si and SiO_2 peaks.[7] Silicon dioxide thickness is given by $t_{ox} = \lambda_{SiO_2} \ln\{[(1/\beta)(I^{exp}_{SiO_2}/I^{exp}_{Si})]+1\}$ for x rays of normal incidence, where λ_{SiO_2} is the attenuation length of the Si $2p$ photoelectrons in SiO_2, $\beta=(I^{\infty}_{SiO_2}/I^{\infty}_{Si})$ is the Si $2p$ intensity from "thick" (>30 nm) SiO_2 and Si, respectively, and $I^{exp}_{SiO_2}/I^{exp}_{Si}$ is the ratio of Si and SiO_2 intensities from the unknown film. We take λ_{SiO_2} to be 2.7 ± 0.02 nm, an average from four references (8–11) and β to be 0.83.[7] With these values and the measured ratio of Si intensities (see first plot of Fig. 1), we calculate that the initial prepared surface has a 1.0 ± 0.1 nm film of SiO_2 on the Si wafer.

The oxide related Si $2p$ core level shift is significantly larger than that of its bulk Si counterpart. Initially, the oxide peak shifts to higher binding energy by 0.35 eV, compared to a shift of 0.15 eV for the bulk Si peak. After oxidation there is a shift to $\sim$1 eV below the initial SiO_2 binding energy. Small shifts are observed with further Ti deposition and oxidation which track the shifts of the bulk Si peak. The approximately 1 eV changes in the relative binding energy of the oxide shifted feature are consistent with Ti silicate formation, i.e., the complete conversion of the interfacial SiO_2 to a Ti silicate alloy, $(TiO_2)_x(SiO_2)_{1-x}$; the value of x will be estimated from core level shifts of the O $1s$ binding energy in Fig. 2.

We note that for the final oxide the intensity of the oxide related Si $2p$ core level has increased relative to the intensity of the substrate related peak. This may indicate either increased oxidation of the substrate or a redistribution of the Si in the oxide layer.

In an effort to determine the band bending of the initial oxidized surface we measured the valence band maximum (VBM) and Si $2p$ core level of a clean, hydrogen terminated Si(100) surface. For a wafer of the same specification as those used in this study we find the Si VBM to be 0.85 eV below the Fermi level, and the Si $2p$ core level at 99.65 eV. This gives an energy difference between the Si $2p$ core level and the VBM of $\Delta E=98.8\pm0.1$ eV. The initial Si $2p$ core level in the thin SiO_2 film (observed at 99.75 eV), in conjunction with this ΔE, places the Si Fermi level at 0.95 ± 0.1 eV above the VBM. The resistivity range of the substrate also gives the bulk Fermi level at 0.9 ± 0.1 eV above the VBM. These results are consistent with flat band conditions after the initial oxidation.

The O $1s$ peak shown in Fig. 2 exhibits a transition from a strong peak at 532.8 eV for the SiO_2 film to an equally strong 530.3 eV peak for the fully evolved TiO_2 film. The peak initially shifts to higher binding energy after the Ti deposition by an amount similar to the observed initial shift

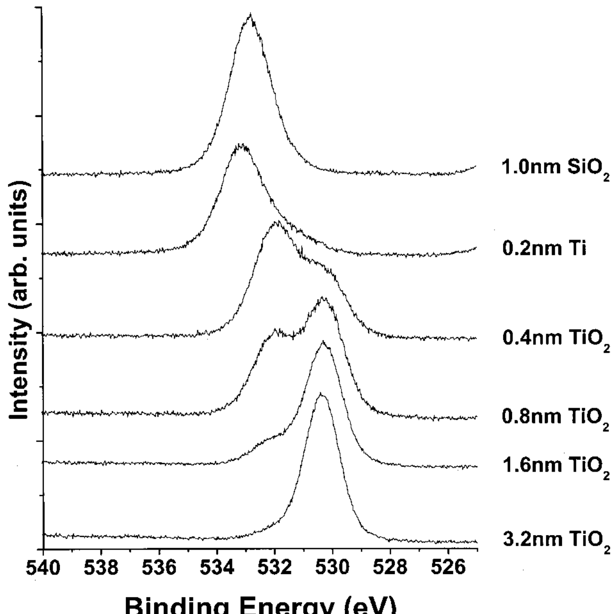

FIG. 2. Oxygen 1s core levels for the prepared surface, initial metal film, and titanium oxides. The sequence runs top to bottom and the labels indicate the total film thickness deposited on SiO_2. Oxygen XPS clearly shows the initial SiO_2, evolving into an intermediate Ti silicate layer before the final product of TiO_2 dielectric film.

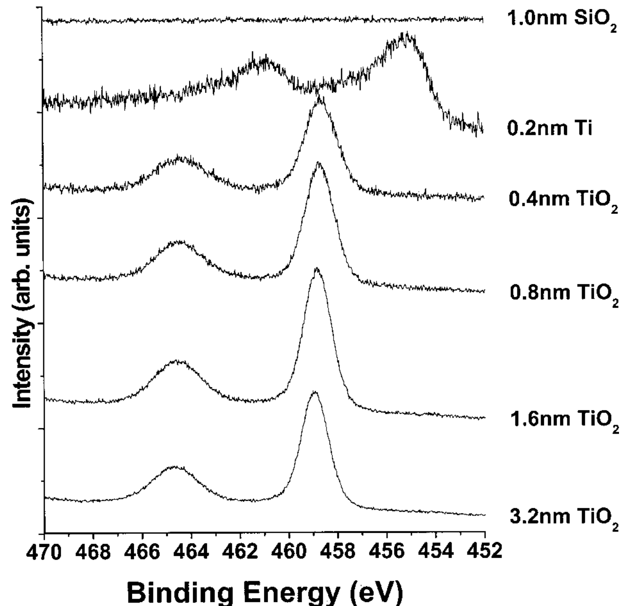

FIG. 3. Titanium 2p core levels for the prepared surface, initial metal film, and titanium oxides. The sequence runs top to bottom and the labels indicate the total film thickness deposited on SiO_2. Shifts of the bound Ti peak in TiO_2 give insight into the field in the oxide layer.

of the oxide related Si 2p peak. After oxidation this peak shifts to 532.0 eV and a second feature is observed that is related to an O–Ti chemical shift. As the Ti oxide thickness is increased, the shifts of the 530.3 eV peak follow that of the Si 2p level. We employ a derived method to determine the TiO_2 film thickness, as no direct measurements are available. The molar densities of Ti, O, and TiO_2 are used to determine the ratio of volumes for Ti and TiO_2. Assuming that the Ti metal is fully oxidized (i.e., two oxygen for every Ti in the final configuration), 1 nm of deposited Ti metal evolves to between 1.8 to 2.0 nm of TiO_2 for the rutile and anatase phases, respectively. Spectra labels reflect the oxide film thickness based on the 2:1 ratio. Low energy electron diffraction (LEED) data shows no diffraction pattern and atomic force microscopy (AFM) imaging shows no discernable grain boundaries and a rms roughness of 0.2 nm.

The O 1s spectra for the TiO_2 of thickness 0.4, 0.8, and 1.0 nm clearly exhibits two features, one at 530.3 eV that corresponds to fully oxidized TiO_2 and a second feature at 532.8 eV, which we assign to a Ti silicate alloy. This is consistent with the evolution of the Si 2p oxide features displayed in Fig. 1. Based on the relative binding energies for SiO_2 and fully oxidized TiO_2 we estimated x, of $(TiO_2)_x(SiO_2)_{1-x}$, the relative TiO_2 concentration, to be approximately 0.4–0.5. This is based on the O 1s binding energy shifts as discussed in Ref. 12.

The titanium 2p1/2 and 2p 3/2 XPS features are displayed in Fig. 3. Initially, there are no features in this energy region, for the prepared SiO_2 surface. After metal deposition, XPS measurements show the two peaks of Ti metal (455.0 and 461.0 eV). After oxidation a large shift is observed for both features, which is attributed to the chemical shift from the oxide formation, giving values consistent with reported values (458.5–459.0 eV).[13,14] As the Ti oxide thickness increases, small shifts are observed, which again follow the shifts of the bulk Si 2p peak. Compared with the changes in the Si 2p peak and the O 1s peak, the results in Fig. 3 demonstrate that the Ti 2p core levels do not show significant shifts in binding energy between Ti silicate and TiO_2 phases. However, the widths of the doublet features for 0.4 nm films and 0.8 nm, in which the Ti silicate fraction is relative large, are broader than those for the TiO_2 film of thickness 3.2 nm. This suggests that there is insufficient resolution to separate the 0.4 and 0.8 nm features into Ti silicate and TiO_2 components.

The ultraviolet photoemission spectra of the initial surface, initial metal film, and after oxidations are displayed in Fig. 4. The strongest feature at $\sim$7.8 eV is largely derived from the O 2p states. The oxide valence band of the initial (SiO_2) surface is determined from a linear fit to the leading edge of the $\sim$7.8 eV feature, which extrapolates to a value of 5.4 eV below the Fermi level. With the formation of the Ti oxide, additional features appear, and the fit to the leading edge is observed at $\sim$3.1 eV.

The UPS spectrum after the initial 0.2 nm Ti deposition (Fig. 5) displays a well-defined turn-on at the Fermi level, and this emission indicates the metallic character of the film. Also, the silicon oxide related features are visible through the thin metal films with the strong feature at $\sim$8.1 eV shifting in binding energy by $\sim$0.3 eV, consistent with the observed shifts in the Si 2p and O 1s features. There is also enhanced emission extending to lower binding energy, which

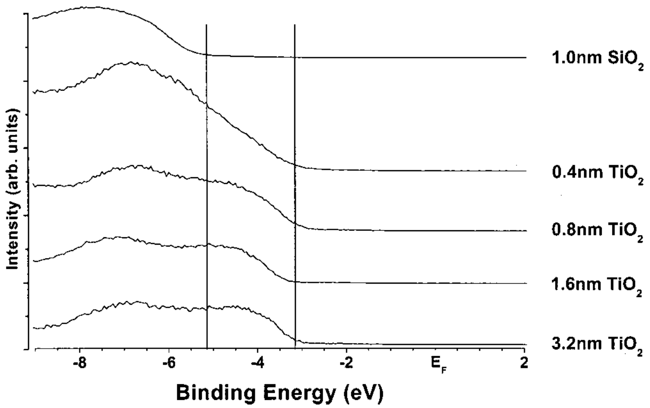

FIG. 4. Valence band spectra for the prepared surface and titanium oxides. The sequence runs top to bottom and the labels indicate the total film thickness deposited on SiO_2. Linear fits of the turn-on give the valence band maximum. Lines indicate VBM for SiO_2 and its shift to the VBM for TiO_2.

FIG. 5. Valence band spectra for the prepared surface and titanium metal. The labels indicate the total film thickness deposited on SiO_2. The metal spectra has a turn on at the Fermi energy and emission characteristic of a metallic film. The oxide valence band maximum is still visible through the metal film.

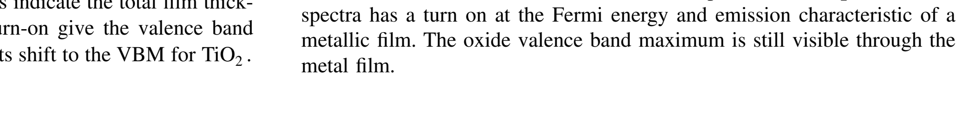

is attributed to some oxidation of the Ti and is probably due to intermixing with the SiO_2.

IV. ANALYSIS AND DISCUSSION

Analysis of the UPS spectra of the initial SiO_2 film finds a valence band maximum at 5.4 eV below the Fermi energy. Based on the 4×10^{16} cm^{-2} doping of the Si, the bulk Fermi level is 0.2 eV below the conduction band minimum. Considering the 1.1 eV band gap of Si, we arrive at a value for the valence band offset of 4.5 eV. With a band gap for SiO_2 of 8.9 eV, the conduction band offset is then 3.3 eV, in reasonable agreement with prior studies.[1] Oxides produced by remote plasma oxidation are found to have low interface state densities ($<10^{11}$ cm^{-2}), which would yield band bending of less than 0.1 eV. We, therefore, assume that the initial oxide has a low interface state density and that the band bending can be neglected.

We can now construct diagrams of the band alignment for the different stages of the development of the interface. Schematic diagrams are presented in Figs. 6 and 7. As noted above, the initial SiO_2 is presumed to have flat bands with less than 0.1 eV of band bending, which implies an interface state density of less than 6.5×10^{10} cm^{-2}.

After deposition of a thin Ti layer, the system equilibrates by charge transfer between the metal and the Si substrate. As indicated in Fig. 7(b), the Fermi levels of the metal and the bulk of the Si align, and charge transfer results in a field in the oxide. The Si core levels shift to higher binding energy by $\sim$0.15 eV, indicating downward band bending. The oxide features have shifted by $\sim$0.5 eV. Subtracting out the shift in the bulk Si core level (band bending) shows that the potential on the oxide results in an average shift of 0.35 eV. Assuming 1.0 nm for the oxide thickness, the 0.7 V (2×0.35 V) across the oxide results in a field of 1.8×10^{8} V/m.

Following oxidation of the metallic layer, the oxide re-

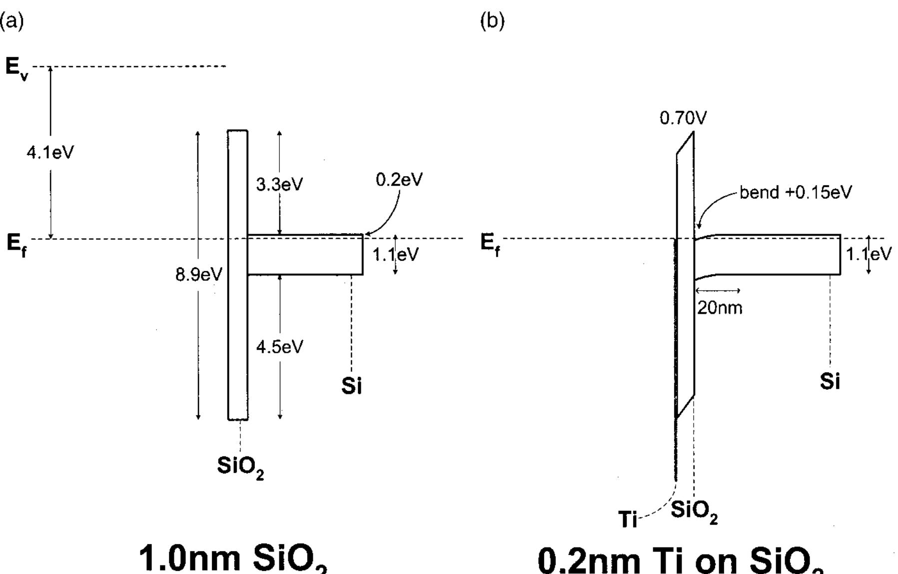

FIG. 6. Schematic band diagram for as deposited SiO_2 (a) and after deposition of 0.2 nm of titanium metal (b). The band alignment for the initial oxide (a) is in good agreement with prior studies and (b) shows bending of Si bands as well as a potential on the SiO_2 layer.

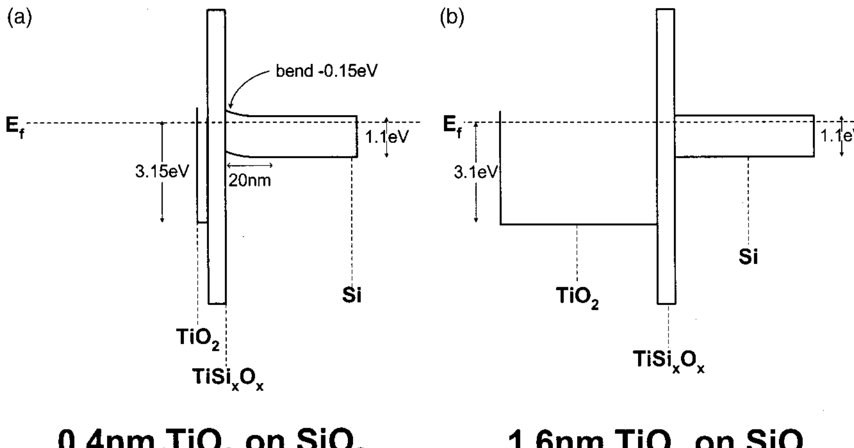

FIG. 7. Schematic band diagram of the first deposited titanium oxide layer (a) and of the final oxide structure (b). The initial titanium oxide (a) shows band bending in the Si substrate with no potential on the oxide layer. The final oxide film (b) shows flat bands and also has no potential on the oxide. The conduction band is not shown because although the position is known to be above Fermi energy, absolute position is not clearly defined by this study.

lated states are observed at ~3.2 eV, and a slight upward band bending of ~0.1 eV can be deduced from the shift of the core levels. It is presumed that there is no significant field in the oxide, and the upward band bending is due to interface states or states in the oxide gap. It is very likely that the Ti has at least partially intermixed with the SiO_2, but without details the schematic in Fig. 8(a) displays the two oxide layers as distinct. It is possible that the states responsible for the band bending originate from this intermixing.

With continued Ti deposition and oxidation, TiO_2 becomes dominant and flat bands are observed in both the Si and the oxide. This structure is shown schematically in Fig. 8(b). The Ti-oxide valence band is found at ~3.1 eV below the Fermi level, which, when taking a band gap of 3.2 eV, puts the TiO_2 conduction band in essential alignment with the conduction band in bulk Si. According to Robertson, Si and TiO_2 display charge neutrality levels (CNLs) at 0.2 and 2.2 eV above their respective VBM. If the band alignment is determined by the CNL, then it is anticipated that the VBM of the TiO_2 would be 2.0 eV below the Si VBM, in agreement with our experimental results.

Figures 6 and 7 do not include conduction bands for the Ti and TiO_2 films. The band gap of thin film TiO_2 is not well known but studies have been done finding a range of values (3.0 to 4.9 eV), depending on phase and preparation technique.[4,5] Taking this range as the band gap for our TiO_2 film these results may explain prior studies of device structures that showed large leakage currents.[15,16] These results imply that the conduction band is above the Fermi level as we see no sign of electrons in the conduction band, however, the absolute position of the oxide conduction band cannot be clearly defined from this study.

Figure 8 displays the valence band density of states as obtained from UPS studies and the relative average energies of the $2p$ O: (i) nonbonding π states (0.0 eV); (ii) bonding π states (-1.6 eV); and (iii) bonding σ states (-6 eV) valence band features obtained from the *ab initio* calculations of Fig. 9.[17] The agreement between the calculated energies and spectral features is excellent. The calculations predict that the corresponding valence band states for Zr–O bonding will be at 0.0, -0.97, and -5.30 eV, respectively. UPS experiments are in progress in our group to obtain the valence

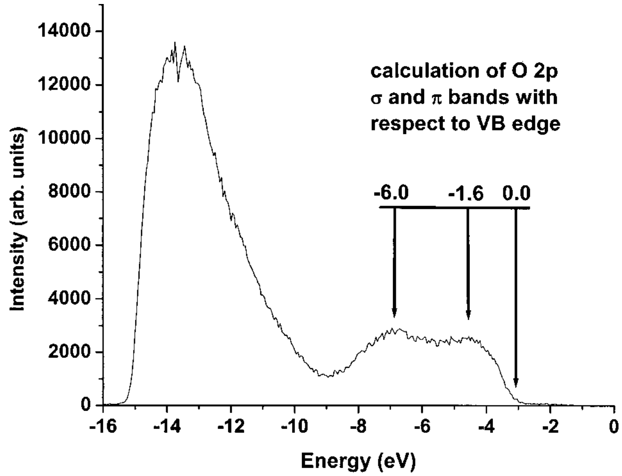

FIG. 8. Final TiO_2 UPS spectra and a comparison between the valence band structure and *ab initio* calculations.

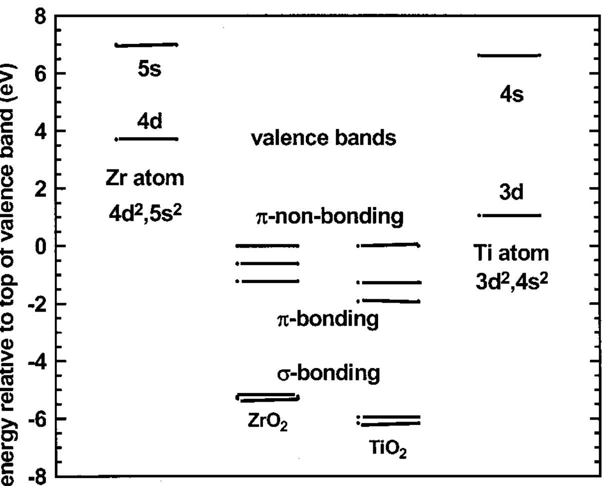

FIG. 9. Atomic state energies and the valence band structures for ZrO_2 and TiO_2 from *ab initio* calculations.

band density of states for ZrO_2 following the same experimental procedures as we have used for TiO_2. Measurements of Miyazaki *et al.* in Ref. 18 give an effective valence band width for ZrO_2 of approximately 5 eV for deposited ZrO_2 films, in good agreement with the *ab initio* results of Fig. 9.

V. CONCLUSIONS

The results presented here show the development of the electronic band structure of oxidized Ti on an oxidized Si surface. The 1.0 nm layer of SiO_2 shows a VB offset of 4.5 eV and essentially flat bands indicating a low density of interface states. Deposition of Ti on the surface results in downward band bending and the presence of a field in the oxide. When the Ti layer is oxidized, a slight upward band bending is observed that is attributed to defects in the oxide. The development of thicker layers of Ti followed by oxidation leads to flat bands and the Ti-oxide VBM is 2.0 eV below the Si VBM, in agreement with the model presented by Robertson.[19]

It was noted that an optimal high K dielectric should have a low interface state density and a band offset to block both holes and electrons.

The results of this study confirm a relatively small conduction band offset between Si and TiO_2, less than 1 eV. This is too small for gate dielectric applications, confirming the results of previously reported studies which have incorporated TiO_2 in metal–oxide–semiconductor devices.[15,16] However, the flat band conditions suggest that the structures can be prepared with a low density of interface states.

Titanium silicates are expected to exhibit a larger band gap and it is possible that an interface structure could be engineered that blocks both electrons and holes, while still maintaining a low interface state density and high K. Future studies are planned to explore these aspects.

ACKNOWLEDGMENT

This work is supported through the Semiconductor Research Corporation, Office of Naval Research, Air Force Office of Scientific Research.

[1] J. W. Keister, J. E. Rowe, J. J. Kolodziej, H. Niimi, T. E. Madey, and G. Lucovsky, J. Vac. Sci. Technol. A **17**, 1250 (1999).
[2] S. A. Campbell, H. S. Kim, D. C. Gilmer, B. He, T. Ma, and W. L. Gladfelter, IBM J. Res. Dev. **43**, 383 (1999).
[3] R. C. Smith, C. J. Taylor, J. Roberts, N. Hoilien, S. A. Campbell, and W. L. Gladfelter, Mater. Res. Soc. Symp. Proc. **611**, C2.8.1 (2000).
[4] N. Rausch and E. P. Burte, J. Electrochem. Soc. **140**, 145 (1993).
[5] J. Pascual, J. Camassel, and H. Mathieu, Phys. Rev. B **18**, 5606 (1978).
[6] T. Yasuda, Y. Ma, S. Habermehl, and G. Lucovsky, J. Vac. Sci. Technol. B **10**, 1844 (1992).
[7] J. R. Shallenberger and D. A. Cole, Proceedings of the 12th Conference on Ion Implantation Technology, 1998.
[8] D. Rob and M. Maier, Fresenius J. Anal. Chem. **333**, 488 (1989).
[9] M. F. Hochella and A. F. Carim, Surf. Sci. Lett. **197**, L260 (1988).
[10] F. Yano, A. Hiraoka, T. Itoga, H. Kojima, K. Kanehori, and Y. Mitsui, J. Vac. Sci. Technol. A **13**, 2671 (1995).
[11] Z. H. Lu, J. P. McCaffrey, B. Brar, G. D. Wilk, R. M. Wallace, L. C. Feldman, and S. P. Tay, Appl. Phys. Lett. **71**, 2764 (1997).
[12] G. B. Rayner, Jr., D. Kang, Y. Zhang, and G. Lucovsky, J. Vac. Sci. Technol. B, these proceedings.
[13] D. Simon, C. Perrin, and J. Bardolle, J. Microsc. Spectrosc. Electron **1**, 175 (1976).
[14] V. I. Nefedov, D. Gati, B. F. Dzhurinskii, N. P. Sergushin, and Y. V. Salyn, Zh. Neorg. Khim. **20**, 2307 (1975).
[15] G. Wilk, R. W. Wallace, and J. M. Anthony, J. Appl. Phys. **89**, 5243 (2001).
[16] S. A. Campbell, D. C. Gilmer, X. Wang, M. T. Hsich, H. S. Kim, W. L. Gladfelter, and J. H. Yan, IEEE Trans. Electron Devices **44**, 104 (1997).
[17] G. Lucovsky, Y. Zhang, R. B. Rayner, and J. L. Whitten, PCSI, 2002.
[18] S. Miyazaki, M. Narasaki, M. Ogasawaga, and M. Hirose, Microelectron. Eng. **59**, 373 (2001).
[19] J. Robertson, J. Vac. Sci. Technol. B **10**, 1785 (2000).